

Supplementary Information

Better Together: Integrating Adhesion and Ion Conductivity in Composite

Binders for High-Performance Silicon Anodes

*Anjali N Preman,^a Suraj Aswale,^a Tejaswi T Salunkhe,^b Seungjae Lee,^a Min Chan Kim,^a Subramani Devaraju,^c Kyu Hyun,^a Hyun-jong Paik,^{*a} Il Tae Kim,^{*b} and Suk-kyun Ahn^{*a}*

^aSchool of Chemical Engineering, Pusan National University, Busan 46241, Republic of Korea

^bDepartment of Chemical, and Biological and Battery Engineering, Gachon University, Seongnam-si, Gyeonggi-do 13120, Republic of Korea

^cPolymer Engineering Laboratory, Department of Chemistry, PSG Institute of Technology and Applied Research, Neelambur 641062, Coimbatore, India.

*E-mail: hpaik@pusan.ac.kr (H-j. Paik), itkim@gachon.ac.kr (I. T. Kim), skahn@pusan.ac.kr (S-k. Ahn)

Experimental

Materials: 2-Amino-4-hydroxy-6-methylpyrimidine (98%), sodium 4-styrenesulfonate (NaSS, >90%), 2-hydroxyethyl methacrylate (HEMA, 97%), poly(acrylic acid) (PAA, $M_w = 450$ kDa), *N*-methyl-2-pyrrolidinone, and dimethyl sulfoxide (DMSO) were purchased from Sigma Aldrich. 2-Isocyanatoethyl methacrylate (>98%) was obtained from TCI and 2,2'-azobis(isobutyronitrile) (AIBN, 98%) was sourced from Junsei. Si nanoparticles (SiNPs, average particle size of 30 nm, 98.5%) and carbon black (Super P, 99+%) were obtained from MTI Korea and Alfa Aesar, respectively. Graphite powder (Gr) was received from Solvay. LiNi_{0.6}Mn_{0.2}Co_{0.2}O₂ powder (NMC622) and poly(vinylidene difluoride) (Solef) were obtained from U&S Plus, Inc. The electrolyte solution (1 M LiPF₆ in ethylene carbonate:ethyl methyl carbonate:diethyl carbonate (30:40:30 v/v/v) containing 10% fluoroethylene carbonate) was purchased from Dongwha Electrolyte.

Synthesis of poly(sodium 4-styrenesulfonate-co-ureido-pyrimidinone methacrylate-co-hydroxyethyl methacrylate) (PSUOH): 2-(3-(6-Methyl-4-oxo-1,4-dihydropyrimidin-2-yl)ureido)ethyl methacrylate (UPyMA) was synthesized as described elsewhere (Fig. S1a).¹ For PSUOH synthesis, NaSS (1.1 g, 53 mmol), UPyMA (0.448 g, 16 mmol), HEMA (0.069 g, 5 mmol), and AIBN (0.003 g, 10 mmol) were dissolved in DMSO (20 mL). The mixture was degassed for 30 min using N₂ and then placed in a preheated oil bath (75 °C), kept there for 15 h, cooled to room temperature, and precipitated in acetone (250 mL). The resulting precipitate was isolated by filtration and vacuum-dried at 40 °C ($M_{n,SEC} \approx 123$ kDa and $\bar{D} = 1.6$). The P(SSNa-co-UPyMA) copolymer (PSU) was synthesized in a similar manner without HEMA ($M_{n,SEC} \approx 151$ kDa and $\bar{D} = 1.6$) (Fig. S1b and Table S1).

Characterizations: ^1H nuclear magnetic resonance spectra were recorded on a Agilent 600 MHz spectrometer (Agilent Technologies) in $\text{DMSO-}d_6$. Molecular weights were determined by size exclusion chromatography (Waters, Alliance e2695) with refractive index detector (Waters 2414) using water as an eluent. Pullulan standards were used to construct a calibration curve. Attenuated total reflectance Fourier transform infrared spectra were collected using a Jasco FT-IR-4600 spectrometer. Differential scanning calorimetry analysis (Discovery DSC 25, TA Instruments) involved heating to $200\text{ }^\circ\text{C}$ followed by cooling to $0\text{ }^\circ\text{C}$ and reheating to $200\text{ }^\circ\text{C}$ at a rate of $10\text{ }^\circ\text{C min}^{-1}$ under N_2 . The viscoelastic properties of crosslinked binder was determined by dynamic mechanical analysis (DMA Q850, TA instruments) using a tension film clamp. A temperature ramp was performed at a rate of $3\text{ }^\circ\text{C min}^{-1}$ from $30\text{ }^\circ\text{C}$ to $200\text{ }^\circ\text{C}$ with a preload of 0.01 N , amplitude of $8.0\text{ }\mu\text{m}$, and frequency of 1.0 Hz . The mechanical properties of the electrodes were evaluated using a nanoindenter (ANTON PAAR Hit 300) at a maximum indentation load of 5.0 mN . The 180° peel test was conducted using a universal testing machine (Dr TECH, DR-100). A 3M tape (1.8 cm in width) was affixed to the laminated side of the electrode and then pulled at an angle of 180° at rate of 40 mm min^{-1} . The force required to strip the laminate from the current collector was recorded. The electrode morphology was analyzed by scanning electron microscopy (Tescan Vega Compact), with each sample coated with a thin layer of Pt ($\sim 8\text{ nm}$) prior to examination. The X-ray photoelectron spectra of the cycled electrodes were recorded using an AXIS SUPRA instrument equipped with an $\text{Al } K_\alpha$ X-ray source (1486.6 eV), and the XPSPEAK 4.1 software was used for peak deconvolution. The rheological properties of the binder solution (10 wt\% in deionized water) were analyzed using an ARES-G2 rheometer (TA Instruments). The measurements were performed using an advanced Peltier system and 40 mm parallel plates, maintaining a temperature of $25\text{ }^\circ\text{C}$ and a gap size of 1 mm . A strain sweep test was performed before the frequency sweep test to obtain the linear viscoelastic region (LVER), and the frequency sweep

test was measured in the angular frequency range 0.1–100 rad s⁻¹. within the LVER obtained from the strain sweep test.

Electrode preparation and cell assembly: Binder solutions with a solid content of 5 wt% were prepared in deionized water (for the Si-Gr electrode) or DMSO (for the Si electrodes). A homogeneous slurry formulated by mixing SiNPs (70 wt%), Super P (15 wt%), and the binder solution (15 wt%) was applied using a doctor blade to fabricate uniform-thickness electrodes, which were vacuum-dried at 80 °C for 12 h. For chemical crosslinking, the Si-PAA/PSUOH electrode was additionally heated at 150 °C for 1 h. The dried electrodes were shaped into 12 mm-diameter discs (area = 1.1304 cm²) and assembled into CR 2032-type coin cells using a Li counter electrode (Shin Hyung E & T, diameter = 14 mm) and polyethylene separator membrane (Wellcos, diameter = 18 mm). The active material loading of the Si electrodes was ~0.7 mg cm⁻². Each cell was supplemented with 200 µL of the electrolyte, sealed, and allowed to sit for 12 h before cycling to ensure the adequate infiltration of the electrolyte into the electrode.

For the Si-Gr electrode, a 1:1 mixture of SiNPs and graphite was subjected to dry mixing in a planetary mixer (AR-100, THINKY). To this Si-Gr active materials (80 wt%), Super P (10 wt%) and the binder solution (10 wt%) were added, and the slurry was continuously mixed. Additional deionized water was added to the slurry at different stages of mixing until the desired viscosity was obtained. During the assembly of LiNi_{0.6}Mn_{0.2}Co_{0.2}O₂ (NMC622)//Si-Gr full cells, the cathode slurry was formulated in *N*-methyl-2-pyrrolidinone by mixing NMC622, Super P, and poly(vinylidene difluoride) in a mass ratio of 90:5:5. The slurry was cast onto battery-grade Al foil and vacuum-dried at 80 °C for 12 h. The active material loading of the NMC622 cathode was maintained at 4.2 mg cm⁻², and the capacity ratio of the

anode/cathode was set at 1.8. Electrode prelithiation was performed in a half-cell configuration prior to full-cell assembly.

Electrochemical measurements: Half-cell galvanostatic charge–discharge tests (WBCS3000L battery cycler, WonATech) were performed in the potential range of 0.01–1.5 V (vs. Li/Li⁺). Full cells were operated at a current rate of 0.05 A g⁻¹ within a potential range of 2.8–4.1 V. Electrochemical impedance spectroscopy and cyclic voltammetry measurements were performed using a ZIVE MP1 station (WonATech). Impedance spectra were recorded at 1.5 V over a frequency range of 100 kHz to 100 mHz and an amplitude 10 mV, and a ZMAN v2.4 simulator was used for impedance parameter regression. A voltage range of 0.01–3.0 V (vs. Li/Li⁺) was chosen for cyclic voltammetry measurements.

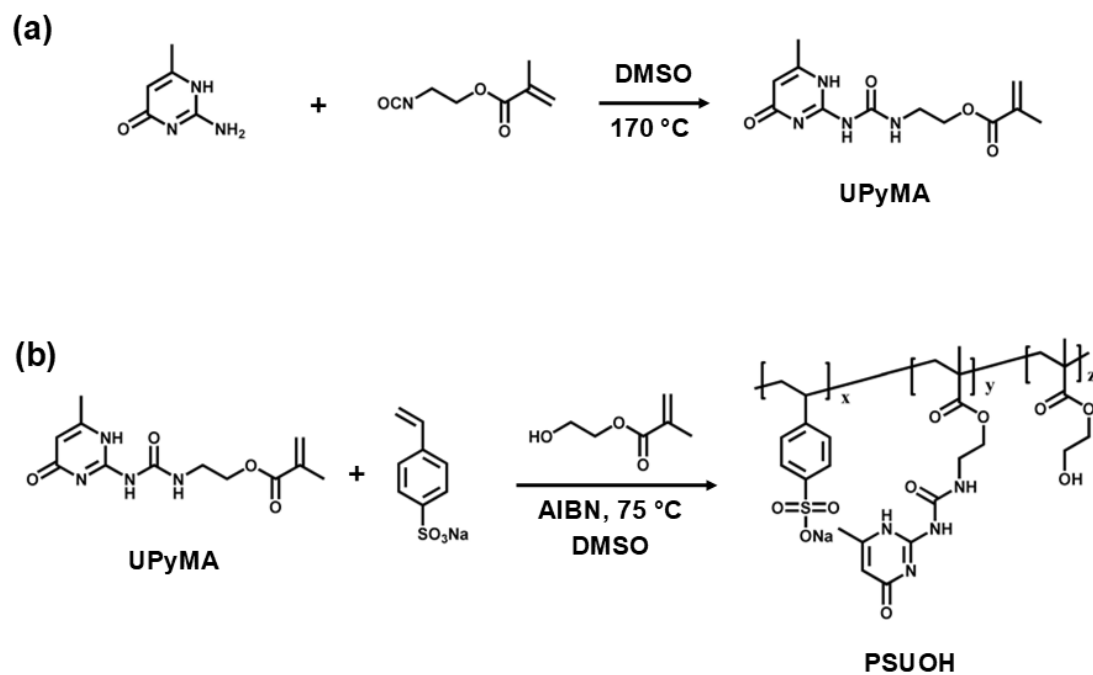


Fig. S1 Syntheses of (a) 2-(3-(6-methyl-4-oxo-1,4-dihydropyrimidin-2-yl)ureido)ethyl methacrylate (UPyMA) and (b) poly(sodium 4-styrenesulfonate-co-ureido-pyrimidinone methacrylate-co-hydroxyethyl methacrylate) (PSUOH).

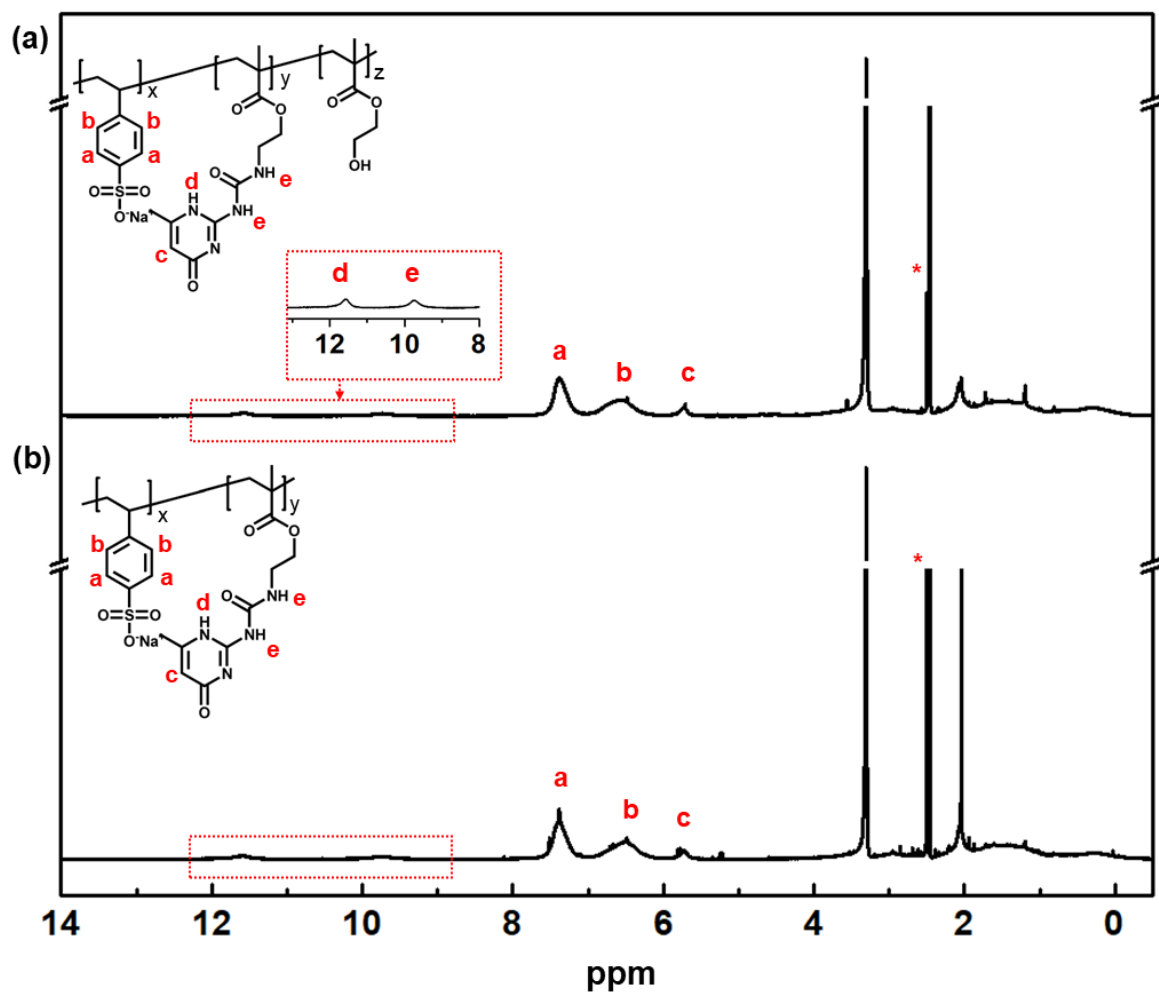


Fig. S2 ^1H nuclear magnetic resonance spectra of (a) PSUOH and (b) poly(sodium 4-styrenesulfonate-co-ureido-pyrimidinone methacrylate) (PSU).

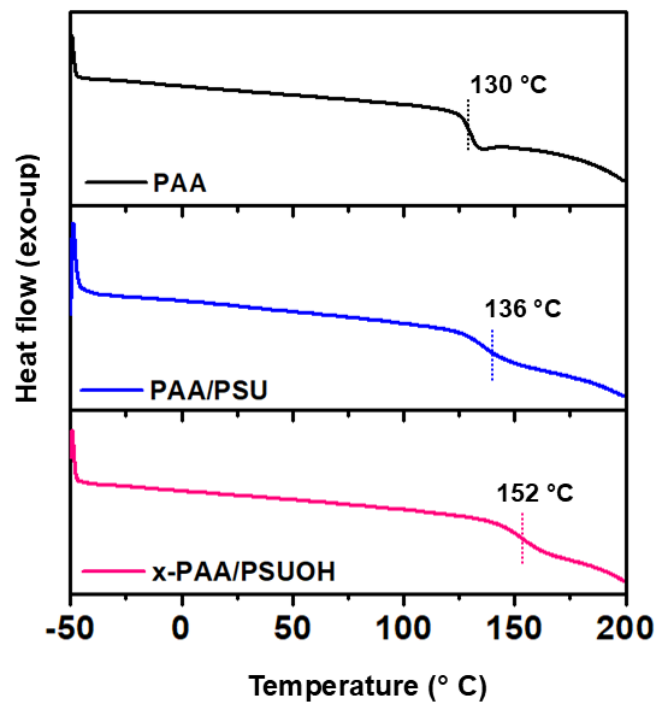


Fig. S3 DSC second heating curves of poly(acrylic acid) (PAA), PAA/PSU, and x-PAA/PSUOH.

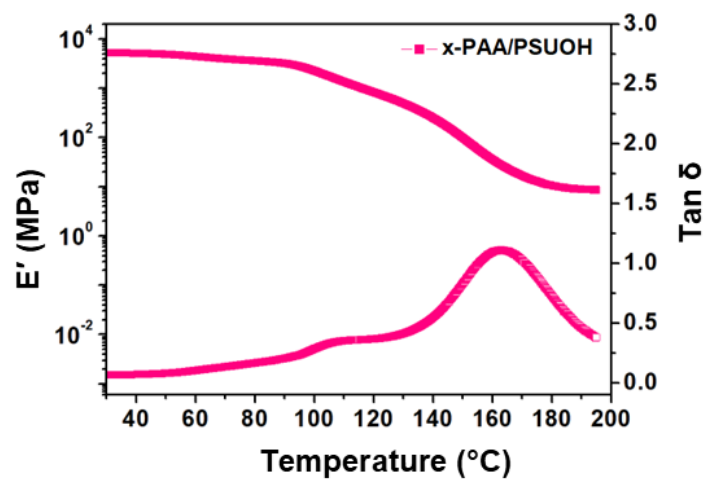


Fig. S4 Storage modulus and tan δ curves of x-PAA/PSUOH during heating.

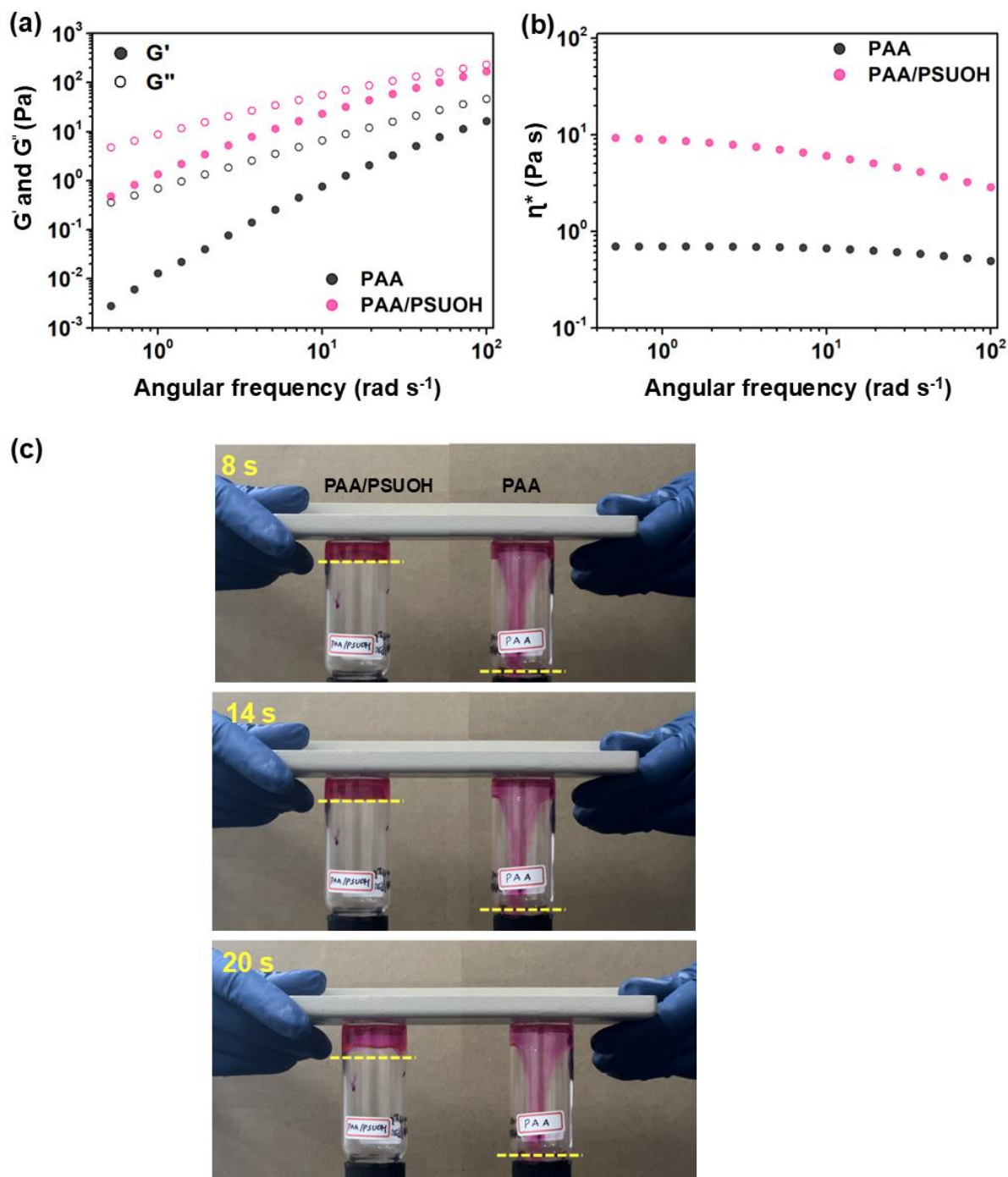


Fig. S5 (a) Storage (G') and loss (G'') moduli and (b) complex viscosities (η^*) of 10 wt% binder solutions in deionized water as functions of the angular frequency. (c) Time-laps photographs of the viscosity flow test captured at designated intervals. Rhodamine was added to the binder solutions to enhance visualization.

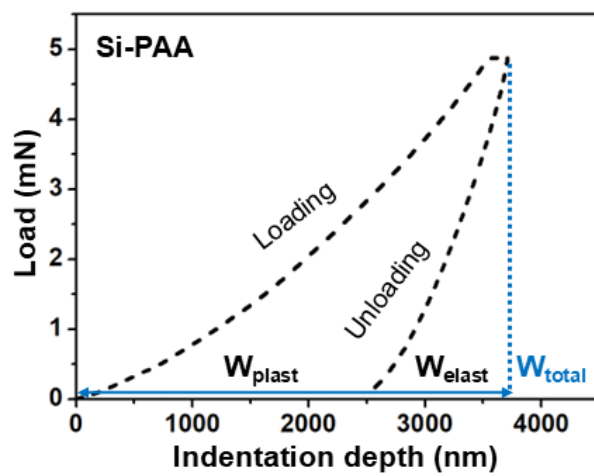


Fig. S6 Load–displacement curve describing the definitions of W_{plast} , W_{elast} , and W_{total} .

Calculation of fracture toughness

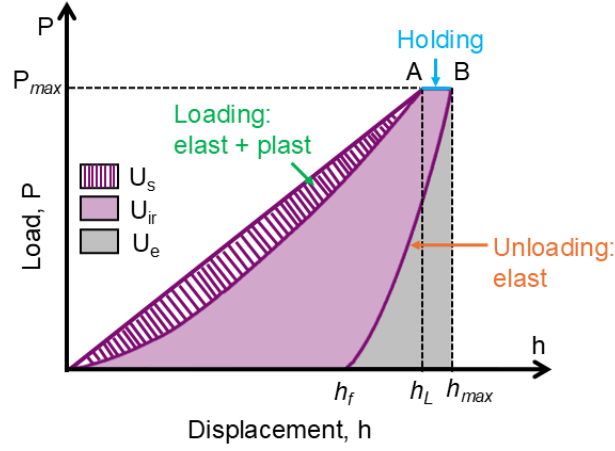


Fig. S7 Nanoindentation load–displacement curve presenting the definitions of U_s , U_{ir} , and U_e .

The fracture toughness of the electrode was obtained from the results of the nanoindentation test as follows.²

Fracture toughness (K_c),

$$K_c = (G_c E_r)^{1/2}, \text{ where } G_c = U_c / A_{max};$$

- $U_c = U_{ir} - U_{pp} = U_t - U_e - U_{pp}$,
- $U_t = \int_0^{h_{max}} p_c dh_c = (p_{max} h_{max})/3$,
- $U_{pp} = U_t - U_t \left[\frac{1 - 3\left(\frac{h_f}{h_{max}}\right)^2 + 2\left(\frac{h_f}{h_{max}}\right)^3}{1 - \left(\frac{h_f}{h_{max}}\right)^2} \right]$
- $A_{max} = 24.5h_{max}^2$

G_c Critical energy release rate, $N m^{-1}$

E_r Reduced Young's modulus, Pa

U_c Fracture energy, N m

A_{max} Maximum contact area, m^2

U_{ir} Irreversible energy, N m

U_{pp} Energy lost during pure plastic stage, N m

U_t Total fracture energy, N m

U_e Elastic energy, N m

h_{max} Maximum displacement, m

p_c Load, N

h_c Contact depth, m

p_{max} Maximum load, N

h_f Residual depth, m

h_L Initial displacement, m

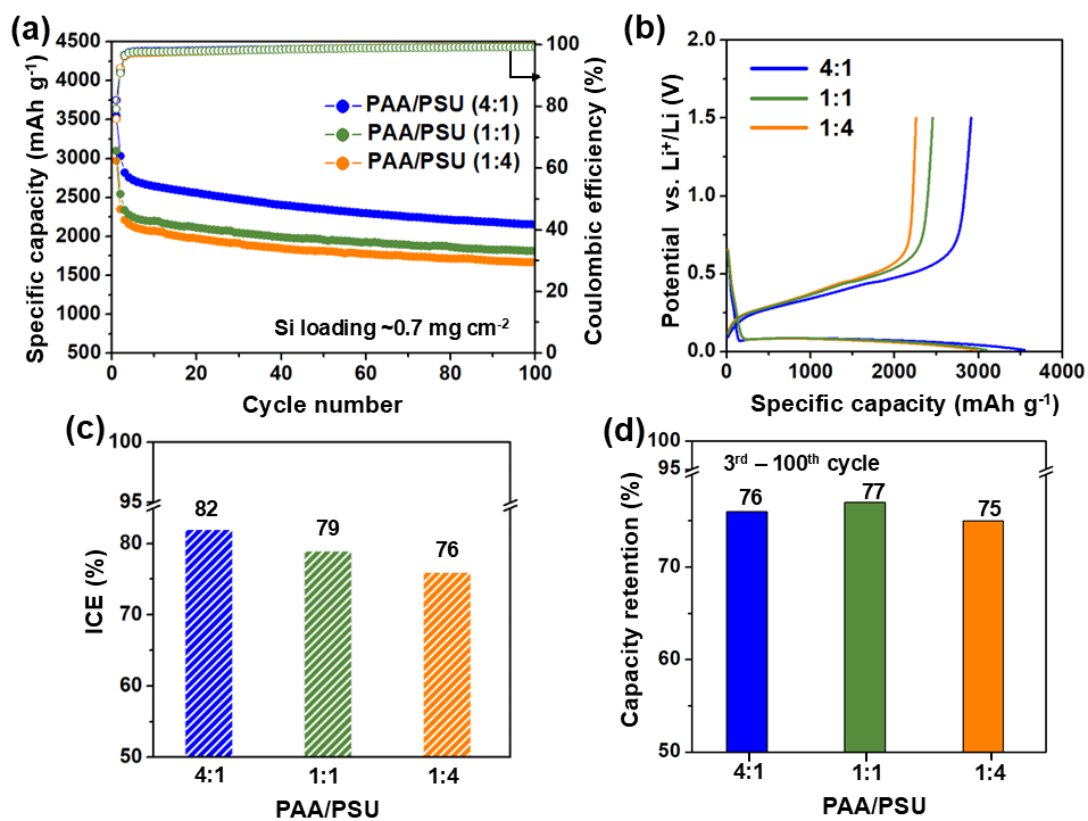


Fig. S8 (a) Cycling performances, (b) initial voltage profiles, (c) initial coulombic efficiencies, and (d) capacity retentions after 100 cycles of Si-PAA/PSU ($x:y$) anodes ($x:y$ = PAA:PSU weight ratio) at 1.0 A g⁻¹.

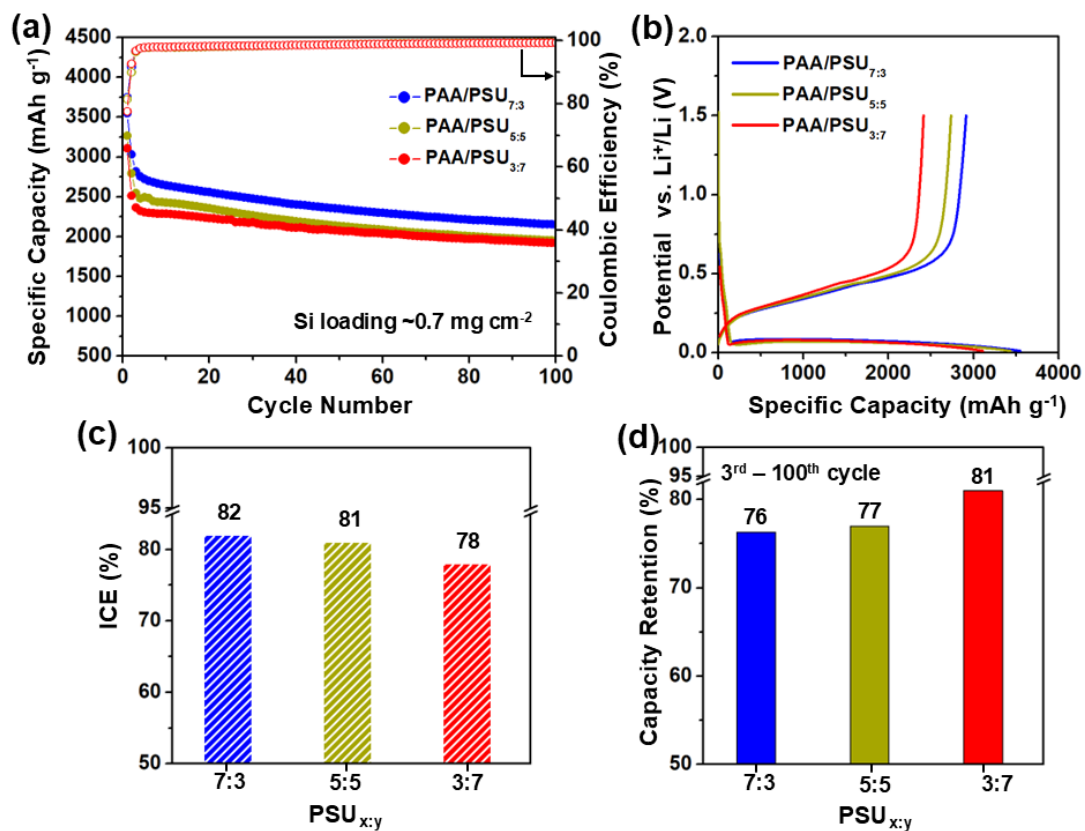


Fig. S9 (a) Cycling performance, (b) initial voltage profiles, (c) initial coulombic efficiencies, and (d) capacity retentions after 100 cycles of Si-PAA/PSU_{x:y} anodes (x:y represents the molar ratio of NaSS to UPyMA in the copolymer) at 1.0 A g⁻¹.

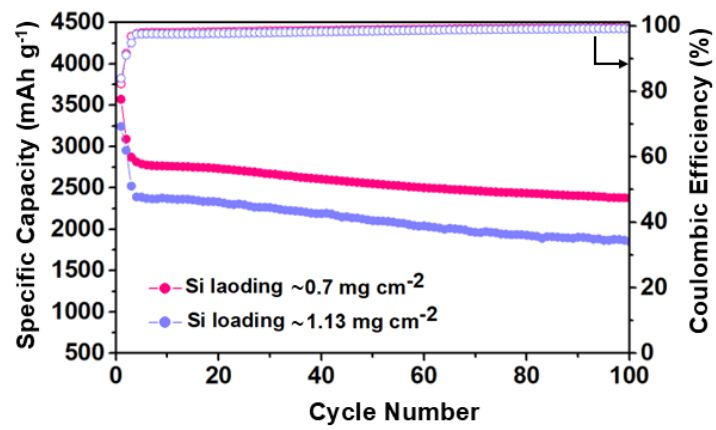


Fig. S10 Cycling performance of Si-x-PAA/PSUOH at different mass loadings under a current density of 1.0 A g⁻¹.

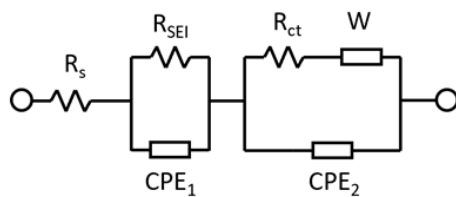


Fig. S11 Equivalent circuit model used for the regression of various impedance parameters. R_s , R_{SEI} , and R_{ct} represent the series, solid-electrolyte-interphase (SEI), and charge-transfer resistances, respectively. CPE_1 and CPE_2 are constant-phase elements associated with the capacitance properties of the SEI layer and Si electrode. The Warburg element (W) corresponds to the Li^+ diffusivity of the system.

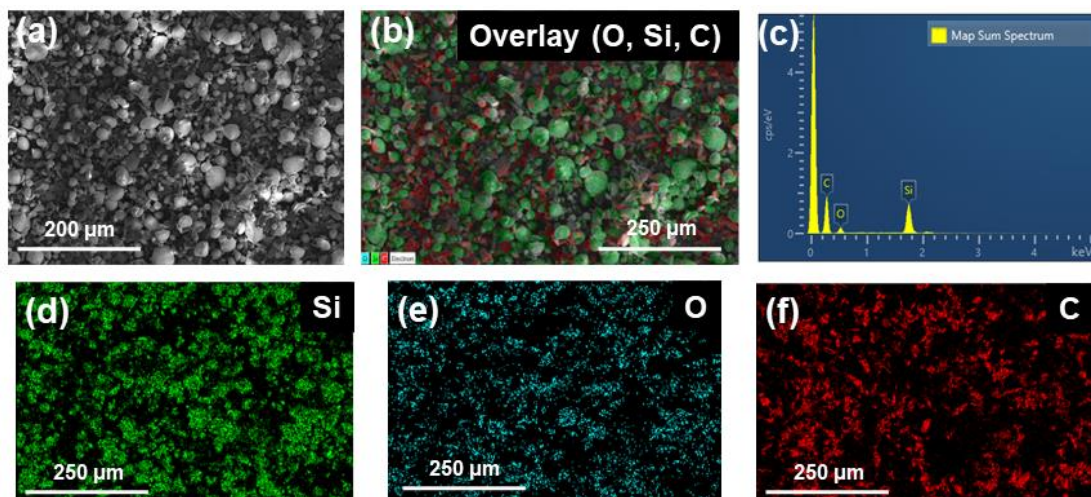


Fig. S12 (a) Scanning electron microscopy and (b–f) energy-dispersive X-ray spectroscopy data of Si and graphite (1:1) after dry mixing.

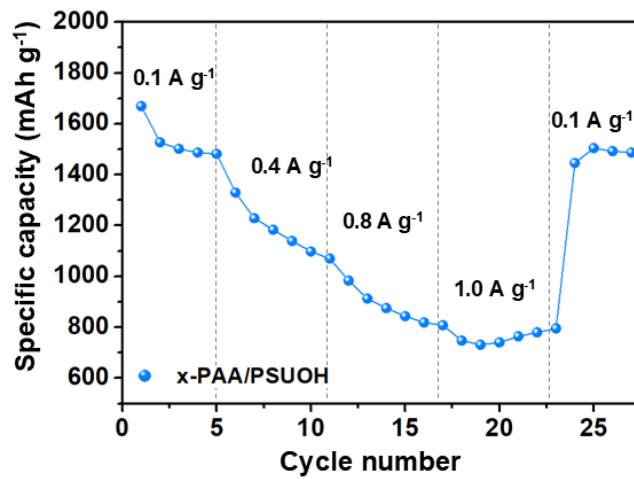


Fig. S13 Cycling performance of the Si/Gr-x-PAA/PSUOH anode at different current rates.

Table S1 Feed ratios used for polymer synthesis, with number-average molecular weights (M_n) and dispersity (D).

	Monomer feed ratio (%)			M_n [kDa]	D
	NaSS	UPyMA	HEMA		
PSUOH	7.1	2.2	0.7	123	1.6
PSU	7	3	-	151	1.6

Table S2 Plastic (W_{plast}) and elastic (W_{elast}) work performed by the indenter during loading–unloading and the corresponding recovery ratio (nit).

Sample	W_{elast} (pJ)	W_{plast} (pJ)	W_{total} (pJ)	nit (%)
Si-PAA	2327.6	4631.2	6958.8	33.4
Si-PAA/PSU	3118.7	2418.5	5537.2	56.3
Si-x-PAA/PSUOH	2465.5	2144.7	4610.2	54

W_{total} = area under the load–displacement (indentation depth) curve recorded during loading.

W_{elast} = area under the load–displacement (indentation depth) curve recorded during unloading.

nit = ratio of elastic work to total work.

Table S3 Electrochemical properties of Si anodes with PAA, PAA/PSU, and x-PAA/PSUOH binders at 1 A g⁻¹. The capacity retention is based on the values at the third and 100th cycles.

Sample	ICE (%)	Specific capacity (mAh g ⁻¹)			Capacity retention (%)
		1 st	3 rd	100 th	
Si-PAA	84	3233	2518	1772	70
Si-PAA/PSU	82	3550	2819	2152	76
Si-x-PAA/PSUOH	82	3572	2871	2377	83

Table S4 Specific capacities and capacity retentions achieved herein compared with those previously reported for other PAA-based blend and composite binders.

Binder	Binder content (%)	Current density (A g ⁻¹)	Si loading (mg cm ⁻²)	No. of cycles	Specific capacity (mAh g ⁻¹)	Capacity retention (%)	Ref.
PAA-DA/PVA	20	0.4	–	100	2507	73	51
PAA-PVA	20	0.4	–	100	2283	63	52
PAA-PU	20	0.84	0.41	200	2253	71	53
PGC	20	2	0.7-0.85	200	1809	74	54
PAA-UPy/5%PEO	20	2.1	0.8-1.5	200	1245	69	55
GE-PAA	10	2.1	0.5	200	1557	67	56
PAA-BFPU	15	2	~1	200	~3000	88	57
PDPP	15	1.78	1.2	100	2312	84	58
PAA-PEO	10	0.84	0.4-0.6	100	2346	59	59
PCI100	10	0.2 C	0.6	300	1745	74.9	60
γ-PGA-PAA	20	0.42	0.7	300	1920	63	61
PPAT-2	15	0.4	0.7–0.9	300	2092.9	73.7	62
x-PAA/PSUOH (This work)	15	1.0	0.7	100 300	2377 2026	83 71	

Table S5 Li⁺ diffusivities calculated based on the cyclic voltammograms of pristine Si anodes with PAA, PAA/PSU, and x-PAA/PSUOH binders.

Sample	D_{Li^+} (cm ² s ⁻¹)	
	Anodic	Cathodic
Si-PAA	4.55×10^{-8}	5.24×10^{-8}
Si-PAA/PSU	6.89×10^{-8}	8.76×10^{-8}
Si-x-PAA/PSUOH	9.2×10^{-8}	9.52×10^{-8}

Table S6 Calculated resistances of Si anodes with PAA, PAA/PSU and x-PAA/PSUOH binders after 50 cycles

Sample	R_s (Ω)	R_{SEI} (Ω)	R_{ct} (Ω)
Si-PAA	5.54	233	888
Si-PAA/PSU	2.65	136	213
Si-x-PAA/PSUOH	2.16	105	186

R_s = Series resistance

R_{SEI} = Resistance of SEI layer

R_{ct} = Charge-transfer resistance

References

1. Y. Song, Y. Chen, R. Chen, H. Zhang, D. Shi, Y. Wang, W. Dong, P. Ma, Y. Zhao, *ACS Appl. Polym. Mater.* **2021**, 3, 2884–2888.
2. X. Shi, S. Jiang, S. Lu, Z. He, D. Li, Z. Wang, D. Xiao, *Petrol. Explor. Dev.* **2019**, 46, 163–172.